# Structural Life Assessment Methods

A.F. Liu

ASM INTERNATIONAL®
The Materials Information Society

First printing, July 1998
Second printing, December 1999



Library of Congress Cataloging-in-Publication Data

Alan F. Liu
Structural Life Assessment Methods
Includes bibliographical references and index.
1. Metals—Fracture
2. Fracture mechanics
3. Accelerated life testing
I. Title
TA460.L59 1998 620.1'66 98-14143
ISBN: 0-87170-653-9
SAN: 204-7586

**ASM International®**
Materials Park, OH 44073-0002

Printed in the United States of America

For a given $K$-level, i.e., for a given crack length and stress level, the distribution of $\sigma_y$ is unchanged whether it is plane stress or plane strain. However, the plastic zone radius for plane stress is three times larger than that for plane strain. Therefore, as far as the effective crack length is concerned, at $(a + r_y)$ the crack undergoes a higher $\sigma_y$ for plane strain than the one for plane stress (see Fig. 1-7). Consequently, the panel that exhibits a higher degree of plane strain will fail first. While further increase of the stress to $S_2$ causes failure in panel $B_4$, panel $B_3$ does not fail, due to the effect of the regions of plane stress (lower crack tip stress) that exist near the specimen surfaces, which are relatively influential in this thinner panel.

Now further assume that at stress level $S_2$ the plastic zone size in panel $B_2$ has reached a dimension equal to its thickness, which implies that plane stress now develops in panel $B_2$. Consequently, further increase of stress will cause failure of $B_3$ first, and then $B_1$, and $B_2$. A rationale has been offered by Broek (Ref 2-5) attempting to explain why $B_1$ should fail first instead of $B_2$. It considers that the local strain in the much thinner sheet $B_1$ is much higher than the strain in $B_2$. As shown in Fig. 1-2, both stress and strain contribute to final fracture of a panel. At stress level $S_4$, the strains in $B_1$ are sufficiently high to cause failure, while $B_2$ can withstand more load and finally fails at $S_5$. Here the thickness $B_2$ can be taken as equivalent to $B_0$ in Fig. 2-4.

## The Phenomenological Aspects of Fracture under Monotonic Loading

Consider the case of a sheet (or a plate) containing a through-the-thickness crack. If loads are applied perpendicular to the crack so that tensile stresses act to open the crack, the level of $K$ increases linearly with the level of the tension stress component normal to the crack. As the level of $K$ increases, some point will be reached at which the crack will start to increase in length. Then the crack will grow to a critical size and onset of rapid crack propagation (fracture) will occur. Schematic illustration of this is given in Fig. 2-9. In practice, the stress at which slow crack growth starts (point 0 in Fig. 2-9) is usually not very well defined. For practical purposes, the stress at the onset of rapid crack propagation (point 1 in Fig. 2-9) may be taken as the maximum stress reached in a test. The critical crack length at rapid fracture is not sharply defined, because the crack length is increasing rapidly up to the length at failure. However, it may be measured to a useful degree of accuracy by observing the fracture appearance of the specimen, or by taking a high-speed motion picture during the test.

Strictly speaking, fracture toughness $K_c$ is computed using critical crack length and fracture load. For engineering purposes, however, a critical $K$-value, i.e., $K_c$, can be computed based on initial crack length and maximum load (point N in Fig. 2-9). This engineering value is often called the $K_{app}$ ($K$-apparent). Therefore, the terminology for critical crack length of a structural part is not clearly defined. Most likely it refers to the criticality of the structural part under consideration. Any critical crack length that is computed using a single value of $K_c$ (which is probably a $K_{app}$ value) is actually the crack length at onset of fracture. However, if desired, the real critical crack length can be determined analytically. We will discuss the technique for doing that in the section "The Crack Growth Resistance Curve" in this chapter.

If the material is ductile and/or the test specimen is in a state of generalized plane stress, slow crack growth is expected to occur. On the other hand,

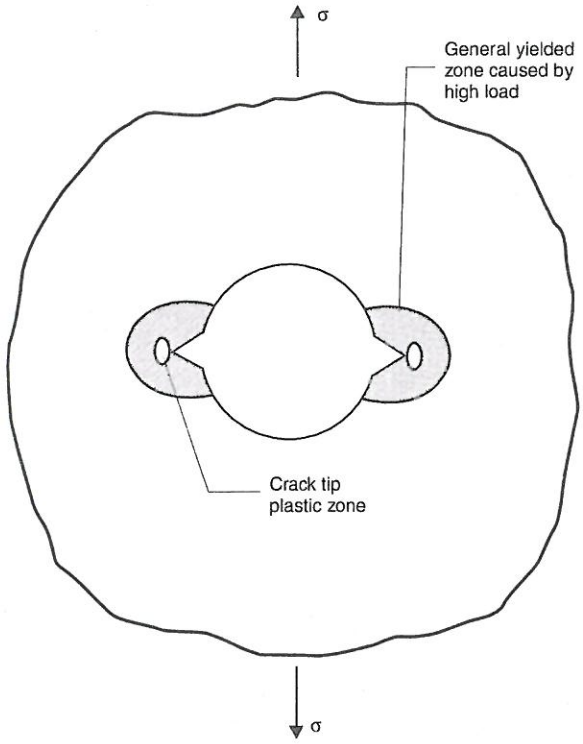


**Fig. 2-11** Small cracks embedded inside a locally deformed zone

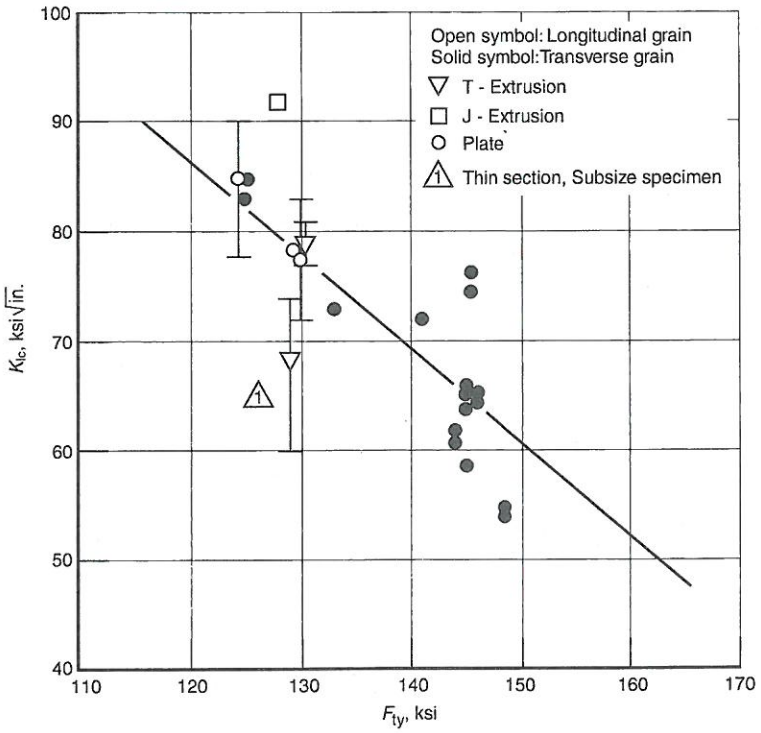


**Fig. 2-12** Plane-strain fracture toughness as a function of material tensile yield strength. Four-point notch-bend specimens. Ti-6Al-4V, mill annealed. Source: Ref 2-6

**Table 2-2 Heat treating methods vs. heat treating operations for D6AC steel**

| Heat treating operation | Heat treating methods | | | | | | | |
|---|---|---|---|---|---|---|---|---|
| | A | B | C | D | E | F | G | H |
| Austenitizing | 1700 ± 25 °F | | 1650 ± 25 °F | | | 1650 ± 25 °F | | |
| Ausbay (interrupted) quenching | Cooled from austenitizing temperature to 975 ± 25 °F in austenitizing furnace and held at 975 ± 25 °F until material is stabilized at this temperature. (Note: Cooling rate between 1350 and 1150 °F must not be less than 6 °F per minute) | | | | | | | |
| Quenching | 140 °F oil | | Salt | | | Salt | | |
| | | | 325 °F | 325 °F | 400 °F | 400 °F | 400 °F | 375 °F |
| Tempering | Double tempered at 1025 °F; held at temperature for 2 h per cycle | | | | | | | |

for the case in which the environment is inert, and temperature, thickness, and other characteristics of the material are such that it is quite brittle, the start of slow crack growth will be followed immediately by the onset of rapid fracture and the obtained fracture toughness will be equivalently plane

**Table 2-3 Summary of D6AC Steel $K_{Ic}$ Data**

| Thickness, in. | Product form | Heat treatment(a) | Avg. $K_{Ic}$, ksi$\sqrt{in.}$ | Number of specimens |
|---|---|---|---|---|
| 0.8 | Forging | E, 400 °F salt | 65.3 | 60 |
| 0.8 | Plate | E, 400 °F salt | 64.5 | 100 |
| 0.8 | Plate | C, 325 ° F salt + agitation | 81.8 | 4 |
| 0.8 | Plate | F, 400 ° F salt | 53.8 | 12 |
| 0.8 | Plate | A, 140 °F oil | 94.6 | 25 |
| 0.8 | Forging | A, 140 ° F oil | 96.9 | 26 |
| 1.5–1.8 | Forging | G, 400 °F salt | 43.8 | 6 |
| 1.5–1.8 | Forging | H, 375 °F salt + agitation | 49.4 | 14 |
| 1.5–1.8 | Plate | H, 375 °F salt + agitation | 61.3 | 20 |
| 1.5–1.8 | Plate | D, 325 °F salt + agitation | 47.0 | 3 |
| 1.5–1.8 | Plate | B, 140 °F oil | 79.1 | 5 |
| 1.5–1.8 | Forging | B, 140 °F oil | 89.6 | 8 |

(a) See Table 2-2 for heat treatment designations

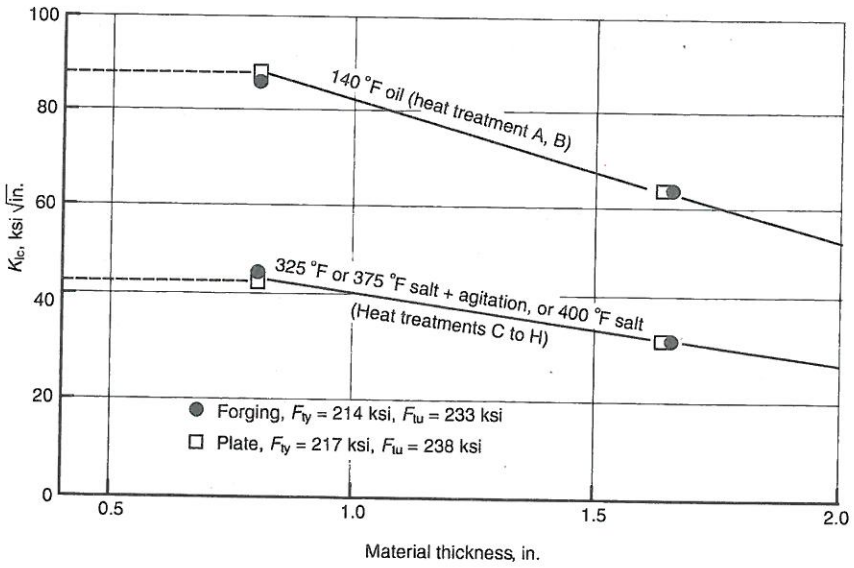


**Fig. 2-13** MIL-HDBK-5 B-scale plane strain fracture toughness values for D6AC steel as a function of heat treatment. Heat treatment designations refer to Table 2-2. Source: Ref 2-10

strain (in magnitude). Thus, the fracture indices are, respectively, $K_c$ or $K_{app}$ for the plane-stress (or mixed-mode) fracture and $K_{Ic}$ for the plane-strain fracture. In reality, it is too complicated to use a real critical crack length to calculate the residual strength (or failure load) by running a computer program for crack growth life prediction. It actually makes more sense to use a $K_{app}$ value, because the crack length at onset of structural failure (i.e., initial crack length) is what is important in structural life/structural damage tolerance prediction.

For a fully embedded flaw (Fig. 2-10a) and the partially exposed flaw (the so-called surface flaw or part-through crack, Fig. 2-10b), the constraint at the leading border of the crack is very high and the mechanism of crack propagation is controlled by a plane-strain condition. Therefore, it is customary to use the $K_{Ic}$ value to predict the residual strength for a surface flaw. Incidentally, the National Aeronautic and Space Administration (NASA) is using an alternate fracture toughness value for routine engineering tasks in the space shuttle program. This fracture toughness value (being called $K_{IE}$) is specifically developed from fracture testing of a surface flaw specimen, because NASA workers found that the fracture behavior of the surface flaw is not entirely the same as $K_{Ic}$. After testing a number of engineering alloys, including aluminum, titanium, steel, Inconel, magnesium, and beryllium-copper, Forman (Ref 2-9) has found that $K_{IE}$ is related to $K_{Ic}$ in the following manner:

$$K_{IE} = K_{Ic} \cdot (1 + C_k \cdot K_{Ic}/F_{ty}) \qquad \text{(Eq 2-2)}$$

where $C_k$ is an empirical constant whose value equals 1.0 $(\text{in.})^{-1/2}$, or 0.1984 $(\text{mm})^{-1/2}$, or 6.275 $(\text{m})^{-1/2}$. However, the relationship of Eq 2-2 is not applicable to very ductile materials (which have a very high $K_{Ic}/F_{ty}$ ratio). The limitation specified by Forman is $K_{IE} \leq 1.4\ K_{Ic}$.

In a real ductile material, if the critical crack depth for a surface flaw is large in comparison with the thickness of the specimen, or if the operating stress level is quite low (for the case of fatigue cycling), then the crack might grow through the thickness before rapid fracture. Once the crack has grown through the thickness, the crack propagation behavior is the same as that of a through-the-thickness crack. Whether it should be called plane-strain or plane-stress failure still depends on the conditions described in the foregoing paragraph.

In summary, $K_c$ failure is associated with a slant fracture appearance with shear lips and slow stable crack growth prior to rapid fracture. The amount of slow stable crack growth depends on the ductility of the material and the

extent of plastic constraint at the crack tip. However, if the material is extremely brittle, rapid fracture may occur without an appreciable amount of slow stable crack growth. This may happen even in a very thin sheet (i.e., in the state of plane stress). An example for 7178-T6 thin aluminum sheet will be shown later in this chapter in the section "The Crack Growth Resistance Curve." The plane-strain fracture index $K_{Ic}$ is associated with a flat fracture appearance without an appreciable amount of crack growth prior to fracture. $K_{Ic}$ is regarded as the minimum value of $K_c$ and is an intrinsic material mechanical property.

Structural details often play an important role in contributing to the residual strength of a structural member. The local area in the immediate vicinity of a stress riser, or a cutout, is known to be susceptible to stress concentration. Taking a circular hole, for example, the local tangential stress at the

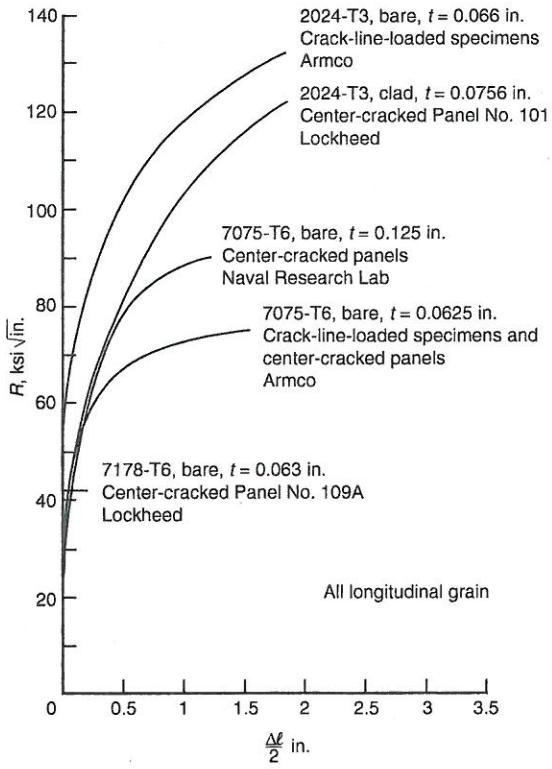


**Fig. 2-14** *R*-curves of aluminum alloys. Source: Ref 2-15 to 2-18

hole edge is at least three times the applied far-field stress. Because the material cannot forever follow Hook's law under monotonic increasing load, in reality it follows the stress-strain relationship of the tensile stress-strain curve. Therefore the magnified stress at the hole edge eventually causes gross-scale yielding around the hole. Depending on the applied stress level,

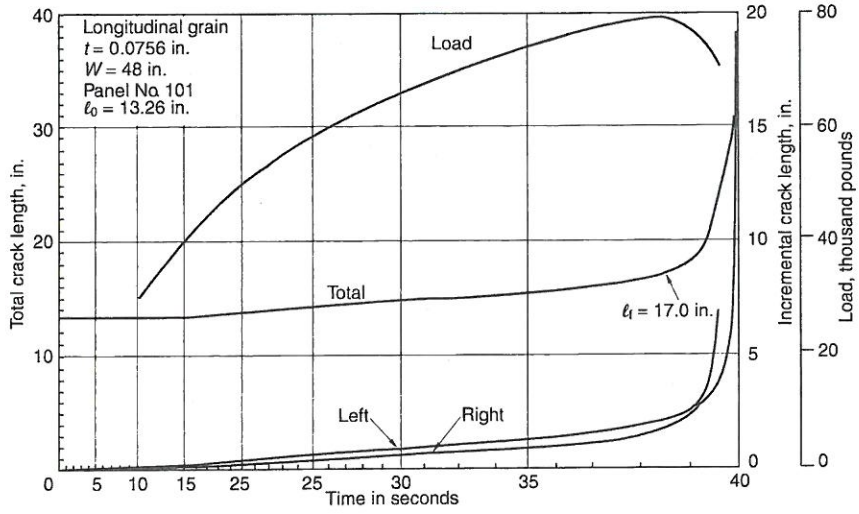


**Fig. 2-15** Crack growth behavior of 2023-T3 aluminum sheet. Source: Ref 2-15

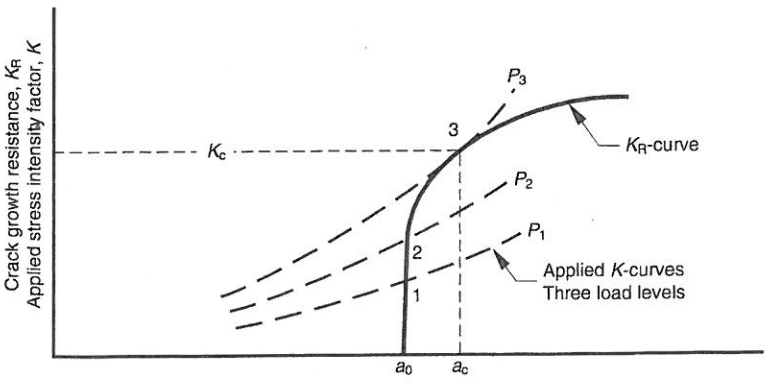


**Fig. 2-16** Schematic representation of superposition of $R$-curve and applied $K$-curves to predict instability. $P_1 < P_2 < P_3$.

the yielded zone adjacent to the hole can be very large, to the extent that a very short crack would be totally embedded inside this zone. A schematic illustration of this situation is shown in Fig. 2-11. It shows that the entire effective crack length (i.e., the physical crack plus the crack tip plastic zone) is embedded inside the locally deformed area. Although this type of fracture behavior has long been recognized, a simple engineering solution to the problem does not exist. Direct application of the current linear fracture mechanics technology to predict the residual strength of this configuration is inappropriate. So far, the $J$-integral is used as an alternate fracture index to characterize fracture behavior involving large-scale yielding at the crack tip. However, Shows et al. have shown that the $J$-integral can also be used to determine the fracture strength of the yielded hole configuration (Ref 2-4). We will demonstrate how this is done in Chapter 8.

Heat treatment and other mechanical (or thermal mechanical) means are known to cause strength variations in a given alloy. The fracture toughness $K_c$ and $K_{Ic}$ of a given alloy are generally found to be inversely proportional to its tensile ultimate or tensile yield strength. A typical example showing the $K_{Ic}$ as a function of tensile yield strength for a titanium alloy is given in Fig. 2-12. For no other reason, heat treatment alone might affect the fracture toughness values of an alloy even if the heat treatments had made no change in tensile strength. To explain what this means, some data for D6AC steel are presented in Tables 2-2 and 2-3 and in Fig. 2-13. These data indicate that the alloy had gone through several different heat treatments but yielded similar tensile strengths. However, depending on the heat treatment, its fracture toughness could have been different by a factor of 2. These data were reported as $K_{Ic}$, however, their values still depend on thickness.

Normally, three basic factors contribute to a brittle cleavage type of fracture: triaxial state of stress, low temperature, and fast loading rate. Although not all three of these factors have to be present at the same time, the conventional dynamic test methods used for determining the ductile-to-brittle transition behavior do involve all these elements. The Charpy and Izod tests (Ref 2-11, 2-12) and the drop-weight test being used by the Naval Research Laboratory (Ref 2-13, 2-14) are typical examples. In fracture mechanics testing, however, it has been shown that loading rate does not affect the fracture toughness of aluminum alloys. An increase in loading rate results in lower $K_c$ for low-carbon steels, but higher $K_c$ for titanium alloys (Ref 2-6).

Aside from a few exceptions reported in the literature, fracture toughness $K_c$ and $K_{Ic}$ are in proportion to test temperature. An increase in test tempera-

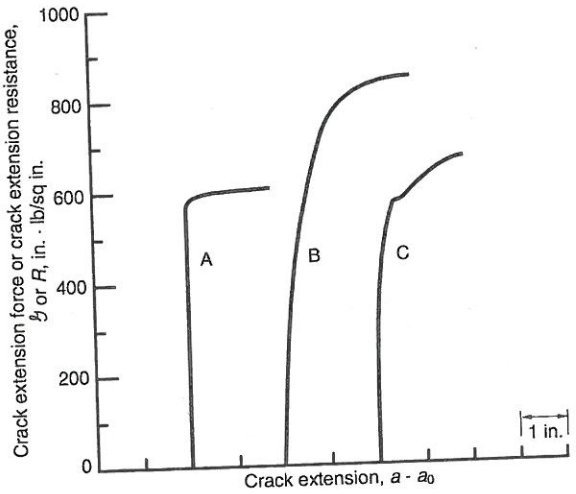


**Fig. 2-17** Some conceivable types of *R*-curves. Source: Ref 2-19

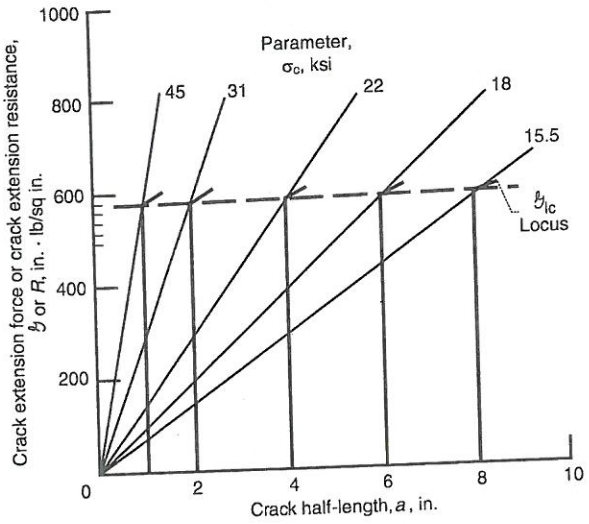


**Fig. 2-18** Crack extension instability condition for various crack lengths in a brittle material. Source: Ref 2-19

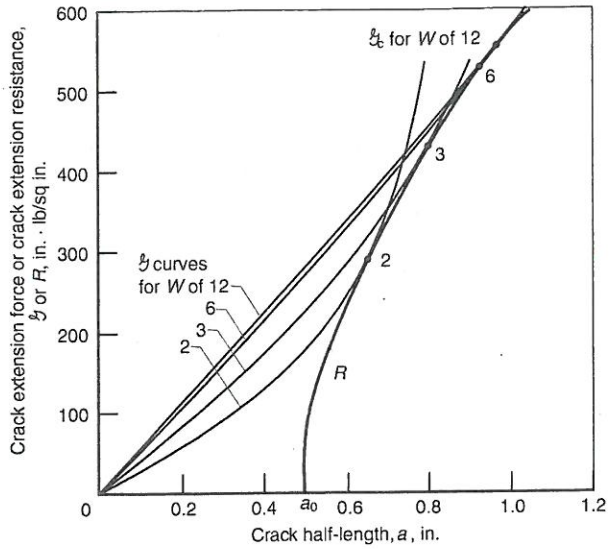


**Fig. 2-19** Dependence of fracture toughness on specimen width, $W$, for center-cracked plate specimens having the same initial half crack length. Source: Ref 2-19

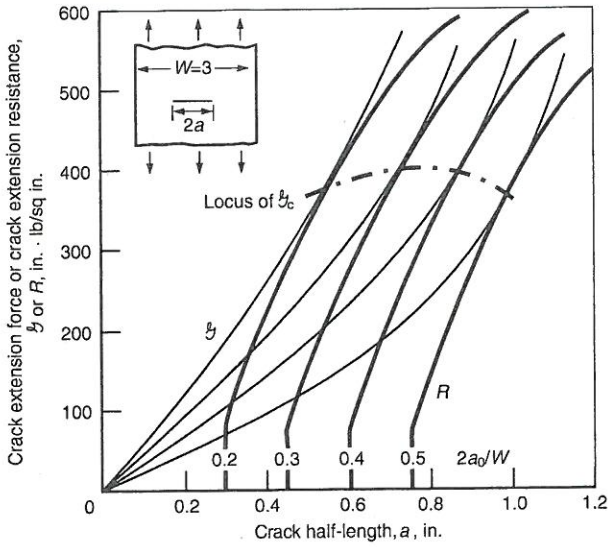


**Fig. 2-20** Dependence of fracture toughness on relative initial crack length for a finite width specimen having an $R$-curve identical to that of Fig. 2-19. Source: Ref 2-19

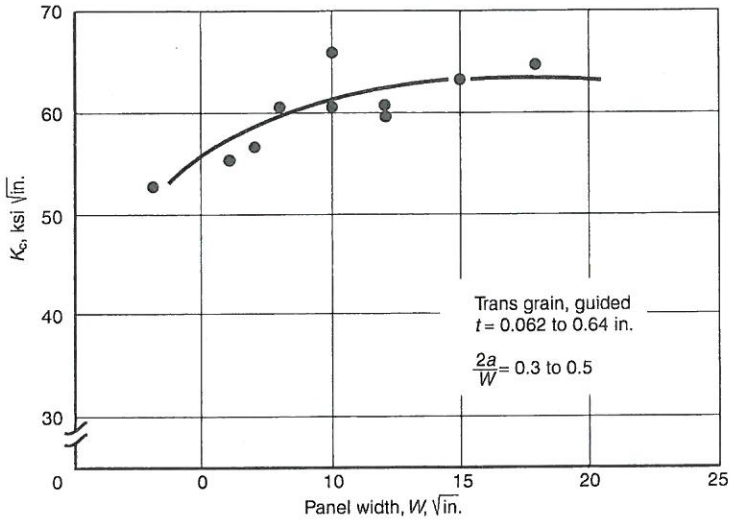


**Fig. 2-21** Effect of panel width on fracture toughness for bare 7075-T6 sheets. Source: Ref 2-20

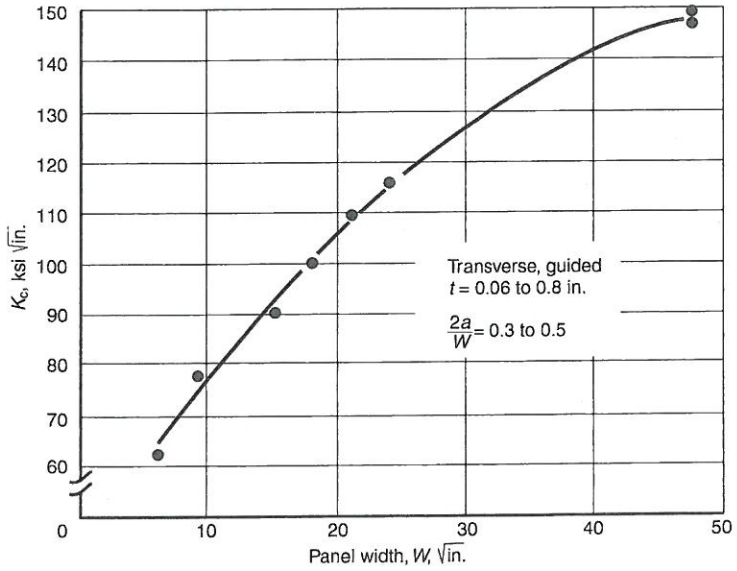


**Fig. 2-22** Effect of panel width on fracture toughness for bare 2024-T3 sheets. Source: Ref 2-20

ture from room temperature normally results in increased fracture toughness associated with decreasing material tensile yield strength. In general, lowering the test temperature leads to an increase in tensile strength coupled with a decrease in crack tip plastic zone size. Consequently, subzero temperatures will cause a normally ductile material to become brittle and thereby exhibit a lower material fracture toughness. This behavior is normally associated with a change from slant fracture appearance to flat fracture appearance. The sensitivity of material tensile strength to low-temperature exposure also depends on crystal structure. Among the three basic types of crystal structures, the body-centered cubic structure, such as in carbon steels, is most susceptible to low temperatures. The face-centered cubic metals, such as aluminum, nickel, copper, and austenitic stainless steels, are much less susceptible to low temperatures.

The effect of corrosive atmosphere probably is not applicable to monotonic load fracture testing, but it applies to fracture testing with a sustained load. We will discuss such behavior in the section "Stress Corrosion Cracking" in Chapter 6.

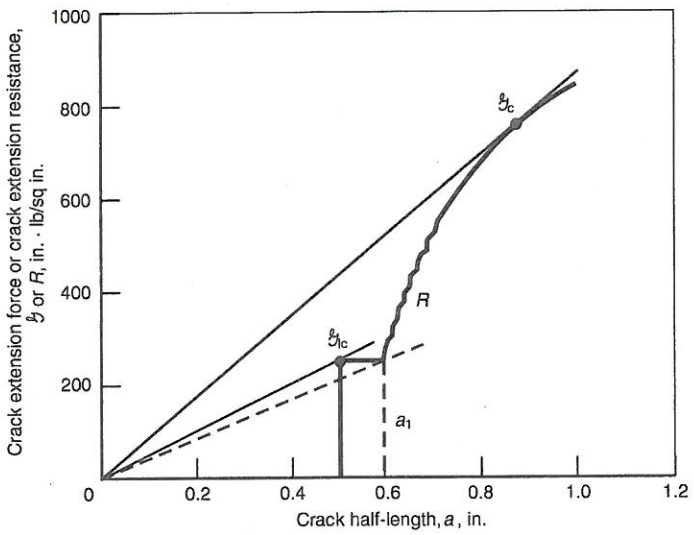


**Fig. 2-23** Meta-instability ($K_{Ic}$) and ultimate instability ($K_c$) for wide plate specimen exhibiting pronounced pop-in behavior. Source: Ref 2-19